electronics

MDPI

Article

Towards 6G Satellite–Terrestrial Networks: Analysis of Air Mobility Operations

Krishnakanth Mohanta † **and Saba Al-Rubaye** *,†

Cranfield University, Bedford MK43 0AL, UK
* Correspondence: s.alrubaye@cranfield.ac.uk
† These authors contributed equally to this work.

Abstract: This paper presents an analytical exploration of sixth-generation (6G) satellite–terrestrial integrated networks, focusing specifically on their applications within air mobility operations, such as those involving unmanned aerial vehicles (UAVs). As the integration of satellite and terrestrial networks promises to revolutionize mobile communication by extending coverage and enhancing connectivity, this study delves into two critical aspects: link budget analysis and handover and mobility analysis for UAVs. The link budget analysis assesses the communication requirements necessary to ensure robust and consistent connectivity between satellites and UAVs, accounting for factors such as path loss, antenna gains, and power transmission. Meanwhile, the handover and mobility analysis investigates the challenges and solutions associated with UAVs transitioning between different network nodes and layers in a dynamic aerial environment. This paper utilizes theoretical models and simulations to provide insights into the design and optimization of these networks, aiming to enhance the reliability and efficiency of UAV operations in the context of the emerging 6G landscape. The findings propose not only technological advancements in network architecture but also practical guidelines for the deployment of UAVs in complex environments, marking a significant step toward the realization of a fully integrated, satellite-terrestrial ecosystem.

Keywords: mobility analysis; handover; 6G; satellite–terrestrial networks; link budget

check for updates

Citation: Mohanta, K.; Al-Rubaye, S. Towards 6G Satellite–Terrestrial Networks: Analysis of Air Mobility Operations. *Electronics* **2024**, *13*, 2855. https://doi.org/10.3390/electronics13142855

Academic Editors: Xin Liu, Zhenyu Na, Min Jia and Lexi Xu

Received: 13 June 2024
Revised: 12 July 2024
Accepted: 17 July 2024
Published: 19 July 2024

Copyright: © 2024 by the authors. Licensee MDPI, Basel, Switzerland. This article is an open access article distributed under the terms and conditions of the Creative Commons Attribution (CC BY) license (https://creativecommons.org/licenses/by/4.0/).

1. Introduction

Urban air mobility (UAM) is a subset of advanced air mobility (AAM), and it is defined as safe and efficient air traffic operations for passenger and cargo transport within the urban environment, with an on-board pilot or a remote pilot in command (RPIC) or a completely autonomous unmanned aircraft system (UAS) [1,2]. Such a technological capability requires a robust communication system (among other systems) capable of operating in a congested urban environment. The UAM system demands a communication system that has good availability, integrity, and security for the safety of its operations in the urban environment.

In this paper, we study the communication systems requirements to support UAM operations. To do so, existing and potential communication systems for UAM are reviewed; they include 3rd Generation Partnership Project (3GPP) 6G technology [3,4]. LEO constellations will be used to provide reliable and fast broadband services to the public in the future and improve communication capabilities and efficiency in various fields [5]. In future 6G technology, space–ground-integrated-network, low-Earth-orbit satellites will play an especially important role [6,7].

Furthermore, this paper elaborates on a performance analysis of the data link for communication between ground stations to unmanned aerial vehicles (UAVs) using link budget analysis and taking weather attenuation and the Doppler effect into consideration. Additionally, the effect of altitude on the quality of service in terms of latency was studied and is presented. These studies will help design robust communication system architectures for UAVs in remote regions.

Urban air mobility (UAM) vehicle operations require specialized communication systems that prioritize robustness and efficiency. Central to these requirements is a resilient command and control (C2) data link, responsible for managing critical flight and safety systems, telemetry data, and communication between the UAM vehicle and the ground station [8–10]. This link must be immune to both unintentional and intentional interference, such as jamming and spoofing, with contingency plans for quick recovery should disruptions occur [11,12]. Additionally, the communication module on the vehicle should be lightweight to conserve energy, thus enhancing the UAV's range and endurance by allowing more power to be allocated to propulsion systems.

UAM communication systems must adapt to the unique challenges posed by the operating environment [13]. They must ensure uninterrupted service across urban [14], rural, or remote terrains at a typical altitude range of 600 to 5000 feet, even necessitating transitions to satellite communications (SATCOM) when terrestrial networks are unavailable [15–17]. Introducing SATCOMs also brings many challenges, including interference management and resource optimization [18–21]. High-speed UAV operation requires the system to accommodate Doppler shifts without failure. Additionally, precise location detection is crucial for collision avoidance, while managing interference is vital to prevent potentially catastrophic failures. To maintain operational efficiency and safety, the system must also support minimal signal losses and low latency, ensuring reliable, real-time communication in urban settings.

Satellite–terrestrial networks employ an architecture that merges the extensive reach of satellite systems with the high capacity and low latency of terrestrial networks [22]. This approach facilitates coverage extension to remote areas and significantly enhances the performance capabilities of Internet-of-Things (IoT) applications; therefore, it is positioned as a backbone for future smart ecosystems [23]. However, despite these advancements, the specific deployment and optimization of these networks for UAV operations pose unique challenges, particularly in maintaining reliable connectivity in dynamic aerial environments. Current research has shown that, while theoretical models for network integration exist, practical applications, especially those involving UAVs, often encounter issues with efficient handover mechanisms and robust link budget management [24,25].

Our manuscript extends this discussion by analyzing the link budget and handover and mobility for UAVs within a 6G satellite–terrestrial framework. This study leverages recent advancements and identifies shortcomings in existing systems to enhance both the theoretical understanding and practical implementation of integrated networks.

The communication system for UAVs and the data links are visualized in Figure 1 below. The introduction of satellite–terrestrial networks could enhance the range of operations of UAVs, especially in remote regions.

Whitworth et al. [26] carried out link budget analysis for 5G communication systems, considering only ground base stations. This paper further extends their study by introducing satellite networks. The contributions of this paper are as follows:

- A detailed link budget analysis for UAV communication within satellite–terrestrial networks. This analysis considers unique factors such as UAV altitude adjustments and atmospheric conditions, which are crucial for ensuring reliable and robust communication links.
- The paper proposes a handover strategy that facilitates seamless network transitions for UAVs.
- Utilizing theoretical models and simulations, the study evaluates the performance of satellite network under various weather scenarios.

Choosing link budget and handover performance analysis for 6G satellite–terrestrial networks targeting UAV operations addresses crucial connectivity needs. Link budget analysis ensures that communication links between UAVs and satellites have adequate signal strength for effective communication, which is crucial for UAVs operating at various altitudes and speeds. Handover performance analysis maintains continuous service as UAVs travel through their designated path, which is crucial for minimizing disruptions during transitions. These areas are interlinked, as a robust link budget underpins stable

connections essential for smooth handovers, thus improving network reliability and service continuity for UAVs in dynamic environments.

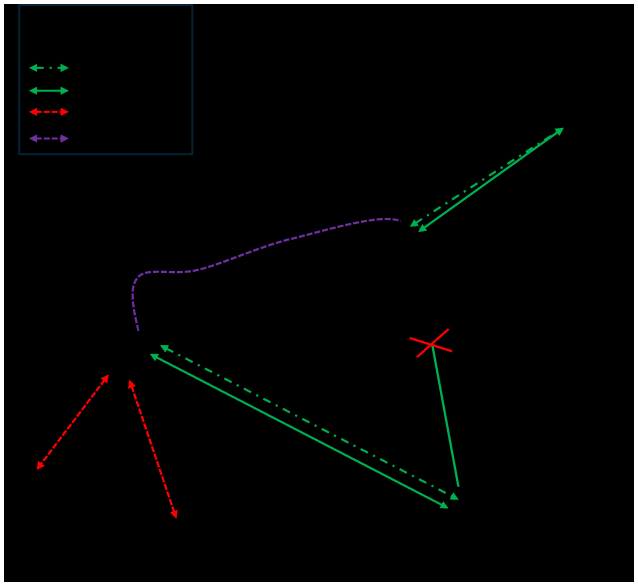

Figure 1. Communication system for UAM.

2. System Architecture

The proposed system architecture integrates 6G satellite and terrestrial networks to support unmanned aerial vehicles (UAVs) in a range of operational scenarios, from commercial deliveries to emergency services. This architecture is designed to leverage the strengths of both satellite and terrestrial technologies, ensuring seamless connectivity, high throughput, and low latency. It includes several key components: a satellite constellation, terrestrial base stations, UAVs as mobile nodes, and a network management system. The system has the following components:

- Satellite constellation: A constellation of low-Earth-orbit (LEO) satellites provides wide coverage and high-bandwidth communication links. These satellites are equipped with advanced beamforming capabilities to dynamically focus connectivity on specific areas or UAVs, enhancing signal strength and reducing interference [27–30].
- Terrestrial network: Comprising 6G base stations, this network layer offers high-speed, low-latency connections in urban and suburban areas [29]. The terrestrial network serves as the primary means of communication where available, with the capability of handing over to the satellite layer when UAVs move out of terrestrial coverage [31].
- UAVs as mobile nodes: UAVs are equipped with dual-mode communication systems capable of connecting to both satellite and terrestrial networks. These systems automatically switch between satellite and terrestrial links based on the signal quality, network load, and predefined operational param.
- Network management system (NMS): This central system coordinates between the satellite and terrestrial networks. It manages resource allocation, monitors network health, and orchestrates handovers between satellites and terrestrial nodes. The NMS uses predictive algorithms to optimize routes and connectivity for UAVs based on their flight plans and network conditions [32].

2.1. System Design

The system design focuses on the following key aspects:

1. Link budget analysis: The link budget is analyzed to determine the maximum range and data throughput achievable under various conditions, including altitude, speed, and weather. This analysis informs the selection of communication technologies and antenna configurations.

2. Signal handover strategy: An effective signal handover strategy is developed to ensure seamless communication continuity as UAM vehicles transition between base-station coverage areas. The entropy method is used to evaluate signal parameters and determine the optimal handover point.

2.2. Testing and Evaluation

The proposed system will be thoroughly tested and evaluated in a simulated environment before deployment in a real-world UAM ecosystem. The testing will focus on the following aspects:

1. Link Performance: Link performance will be measured under various conditions to validate the link budget analysis and ensure that data transmission meets the requirements.
2. Handover Performance: Handover success rate will be evaluated to ensure seamless communication continuity during vehicle transitions.

3. Link Budget Analysis

A link budget analysis is performed to evaluate the feasibility and reliability of the communication system. This analysis involves calculating all the gains and losses encountered along the transmission path to determine whether the signal strength is sufficient for effective communication. This assessment takes into account various factors such as distance, frequencies, antenna gains, weather, and signal losses. [33]

This research explores the following:

- An evaluation of path losses in different weather conditions.
- The effect of altitude on the QoS parameters of the UAV communication system.

The system parameters considered for the study are tabulated below in Table 1.

Table 1. System parameters.

System Parameters	Specification
Operating (center) frequency	3.5 GHz
Antenna gain (drone-mounted)	10 dBi
UAM vehicle velocity	45 m/s
Polarization	VV (Vertical)
Transmitter cable and connector loss	3 dB
Receiver antenna diameter	1.5 m
Antenna efficiency	75%
Base station power	38 dBm (6G ground station)
Noise temperature	300 K
Rain rate	80 mm/h
Specific attenuation (k)	2 dB/km
Polarization constant (α) (for vertical polarization)	0.07
Specific attenuation for dry air (γ_0)	0.08 dB/km
Specific attenuation for water vapor (γ_w)	0.5 dB/km
Minimum required C/N	−120 dB (for 6G)
Satellite altitude	800 km

The values considered for the analysis were assumed based on a literature review, as no standards have been established for 6G yet [34,35].

3.1. Link Margin

The link margin represents the excess power available, calculated as the difference between the received power (P_{RX}) and the minimum power required for the receiver's reliable communication, known as receiver sensitivity (RS). A positive link margin is essential for the effective establishment of a communication system. The formula for determining the link margin is outlined in Equation (1)

$$LM = P_{RX} - RS \quad (1)$$

3.2. Link Budget Equation

The general link budget equation is shown below (Equation (2)):

$$P_{RX} = P_{TX} + G_{TX} - L_{TX} - L_{FS} - L_M + G_{RX} - L_{RX} \quad (2)$$

where the following applies:

P_{RX}: received power (dBm).
P_{TX}: transmitter output power(dBm).
G_{TX}: transmitter antenna gain (dBi).
L_{TX}: transmitter losses in dB.
L_{FS}: free space path loss in dB.
L_M: other losses in dB.
G_{RX}: receiver antenna gain (dBi).
L_{RX}: receiver losses in dB.

For the given Equation (2), the transmitter power (P_{TX}), transmitter loss (L_{TX}), and receiver antenna gain (G_{RX}) are given in Table 1. To calculate the transmitter gain, the following Equation (3) is used:

$$G_{TX} = 10 \log \left(\eta \times \left(\frac{\pi D}{\lambda} \right)^2 \right) \quad (3)$$

where the following applies:

η: antenna efficiency.
D: antenna diameter.
λ: wavelength.

3.3. Attennuations

The communication system is expected to experience attenuation losses due to the various factors outlined below:

- Free space path loss: An essential component of the link budget analysis, the free space path loss (FSPL) quantifies the reduction in signal strength as it travels through open space unimpeded by any obstacles or interference. The formula for calculating the free space loss (L_{FS}) is presented in Equation (4).

$$20 \log \left(\frac{4\pi d}{\lambda} \right) = 20 \log(d) + 20 \log(f) + 20 \log(4\pi / c) \quad (4)$$

  where d represents the distance between the base station/satellite and the UAS.
- Doppler effect: Given that the UAS will be moving at some speed, the Doppler effect must be considered when determining the received power (P_{RX}). This consideration is incorporated into the formula as depicted in Equation (5), as all the variables in the equation are expressed in dB.

$$P_{RX} = P_{TX} + G_{TX} - L_{TX} - L_{FS} - L_M + G_{RX} - L_{RX} \pm 10log(f_{ds}) \quad (5)$$

  where f_{ds} is the shift in the Doppler effect given in Equation (6):

$$f_{ds} = v_{rel} \frac{f}{c} \quad (6)$$

  v_{rel} is the relative velocity of the UAV with respect to the base station/satellite. In the case of satellites, the relative velocity is considered to be the orbit velocity of the satellite. In Equation (5), the $\pm$ symbol indicates the direction of travel of the UAV—whether it is moving towards or away from the base station. For this particular scenario, it is assumed that the UAV is departing from the base station; therefore, the '$-$' sign is applied.

- Atmospheric attenuation: Atmospheric attenuation, mainly due to atmospheric gases, significantly influences the link budget of communication systems, particularly at higher frequencies. This type of attenuation adds to the total path loss and impacts the strength of the signal that is received.
  The attenuation, represented as γ (dB/km), is determined using the formula shown in Equation (7).
  $$\gamma = \gamma_o + \gamma_w \tag{7}$$
  In this context, γ_o represents the specific attenuation due to dry air, and γ_w signifies the specific attenuation due to water vapor.
  The attenuation of the signal caused by the atmosphere is determined by multiplying the overall specific attenuation, γ, by the distance, d, that the signal travels through the gas. Therefore, the power loss from gas attenuation, denoted as L_{atm}, can be computed using Equation (8).
  $$L_{atm} = \gamma d \tag{8}$$
- Rain attenuation: Rain attenuation is the decrease in signal strength that occurs due to rain in the path of communication. It is a crucial consideration in link budget analysis, particularly for AAM communication systems that operate at frequencies prone to signal weakening caused by rain.
  Rain attenuation is expressed in the following formula (refer to Equation (9)):
  $$A_{\text{rain}} = kR^{\alpha} \tag{9}$$
  In this Equation (9), the following applies:
  - R represents the rain rate in mm/h.
  - k denotes the specific attenuation measured in dB/km.
  - α is the polarization constant, which can differ, based on the polarization orientation.

  k and α are considered to be k_V and α_V for vertical polarization. The scenario presented considers vertical polarisation only.
  The impact of this attenuation on signal losses due to rain can be calculated as shown in the next equation, where v is the vertical component of the distance from the UAV to the base station.
  $$L_{rain} = A_{rain} * v \tag{10}$$

In the case of satellite communications, the rain and atmospheric attenuations are limited to a certain altitude. The rain attenuation happens below the clouds, and the atmospheric attenuation significantly drops beyond the stratosphere. This can be visualized using Figure 2.

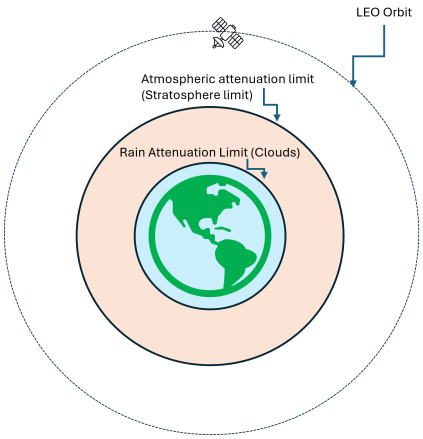

Figure 2. Attenuation limits along the signal path.

3.4. Total Path Loss

The path loss model encompasses all signal losses incurred during propagation from the transmitter to the receiver, essentially aggregating all individual losses. For the specific scenario in question, the path loss can be computed using the following formula:

$$Path\ Loss = FSPL - 10log(f_{ds}) - L_{gas} - L_{rain} \tag{11}$$

In addition to received power, two additional metrics that can be utilized to assess the link budget analysis include the following:

- The carrier-to-noise ratio: This ratio, represented in Equation (12), measures the received carrier strength to the received noise. This is also called the signal-to-noise ratio (SNR).

$$SNR = \frac{P_{RX}}{Noise\ Power\ (N)} \tag{12}$$

- Latency Latency denotes the delay that signals encounter as they pass through a communication system. Although latency is not usually included in standard link budget analyses, it plays a critical role in the planning and performance assessment of communication frameworks, particularly in situations requiring an immediate or time-sensitive exchange of data. The formula for latency (t) is given in Equation (13).

$$t = \frac{Distance\ (d)}{c} \tag{13}$$

The latency equation presented does not factor in the UAV's speed. However, in practical scenarios, it would likely be influenced by the processing times at both the transmitter and receiver ends. Since we lack specific data regarding this, we assume that processing occurs instantaneously, without any delay.
These equations are applied to perform the link budget analysis for the given scenario.

4. Communication Handover

Handover refers to the mechanism through which mobile devices transition between networks. In this research, the focus is on UAVs as moving devices. As a UAV travels along its route, it must switch from one network tower (or base station) to another as it enters and exits the coverage areas of these stations. Handovers can be a switching of networks between the same type of network (horizontal handover) or to a different type of network (vertical handover). Vertical handovers also include handovers to non-terrestrial networks like satellite networks and high-altitude platforms (HAPs) to ensure reliable and robust data links with flights and UAVs traveling above remote areas [4,36]. This process is illustrated in Figure 3.

There are many handover strategies discussed and studied for satellites. One of the strategies proposed is by Deng et al. [37], by whom an assisted soft handoff algorithm was introduced, building on the WCDMA system's soft handoff approach and using location information to calculate the residence time. However, this method was proposed for GEO satellites. For LEO satellite-based communication systems, Wu et al. proposed handovers based on a 'potential game' for mobile terminals [38]. There are other strategies for handovers that use the tracking time, signal quality, and maximum separation angle as the decision parameter [39].

While there are multiple handover strategies, entropy-based handovers are preferred for urban air mobility applications [40]. This is because of the following reasons:

- Entropy-based methods can dynamically adjust to changes in various link parameters like the received signal strength, latency, capacity of satellite, etc., reducing the likelihood of dropped connections.

- UAM vehicles, such as drones and air taxis, move at high speeds and altitudes, which require rapid adjustments in network connections. Entropy-based systems can handle these dynamics more effectively than traditional methods [41].
- This method is scalable. When more satellites or parameters are introduced, appropriate weights can be designated for them.

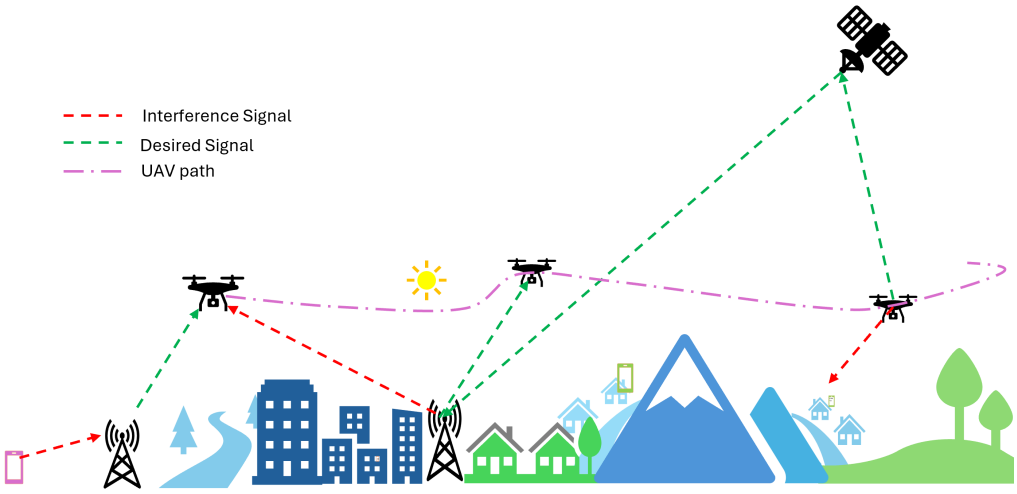

Figure 3. Visualization of handovers.

Entropy-Based Handover

Entropy-based handover calculates the entropy of various handover criteria—such as the signal strength, network load, and user mobility—to determine their respective variability and impact on the network. Criteria with lower entropy (less variability) are considered more stable and are given a heavier weight in the decision-making process. This weighting helps in prioritizing handover targets based on a comprehensive, data-driven evaluation.

The entropy weight method is employed to evaluate the spread of values across various criteria or indices. It quantifies the level of differentiation among these criteria, allocating increased weights to indicators that show more significant dispersion [41].

The mathematical formulation of the entropy method, essential for decision-making in signal handover strategies, is detailed in Equations (14) and (18), as per [40]. The criteria for a handover are as follows:

$$P_{new} > P_{old} + \text{Entropy} \tag{14}$$

Here, (P_{new}) and (P_{old}) represent the power from the new and the old base stations, respectively. The term 'Entropy' in this context is derived from the entropy weight method, illustrated in Equation (15):

$$E_i = -\frac{\sum_{j=1}^{n} p_{ij} \cdot \ln p_{ij}}{\ln n} \tag{15}$$

In this equation, p_{ij} stands for the normalized values for the i^{th} indicator and j^{th} sample, defined as follows:

$$p_{ij} = \frac{x_{ij}}{\sum_{j=1}^{n} x_{ij}} \tag{16}$$

For the analysis, three ground base stations and one satellite were considered. Given that there are four base stations in total ($n = 4$), the specific entropy for signal strength is given as follows:

$$E_i = -\frac{\sum_{j=1}^{4} p_{ij} \cdot \ln p_{ij}}{\ln(4)} \tag{17}$$

i.e.,

$$\text{Entropy} = -\Sigma(p(x)^* \log_4(p(x))) \tag{18}$$

In this analysis, for simplicity, we consider just one indicator, namely the received signal strength (RSS), and with three samples from three base stations. This assumption was made since the study was done for a single satellite. The introduction of new satellites or a constellation of satellites would require inputs of other indicators like the capacity, remaining service time, and satellite load (capacity). The weights for other indicators are not considered, thereby simplifying the weighted entropy method to a basic entropy calculation.

The standardized values of RSS are computed as follows:

$$p_j = \frac{RSS_j}{\sum_{j=1}^{4} RSS_j} \tag{19}$$

This study aimed to develop a signal handover strategy for drones, focusing solely on RSS. The network conditions before and after handovers are illustrated, along with the corresponding signal strengths.

The assumptions for the study include the following:

- A drone travels in a straight flight path along the X-axis.
- The rain and gas attenuation are considered.
- A constant UAV altitude and a velocity of 45 m/s are involved.
- The satellite is on the XY plane
- The drone has an elevation mask of 60°, as shown in Figure 4.

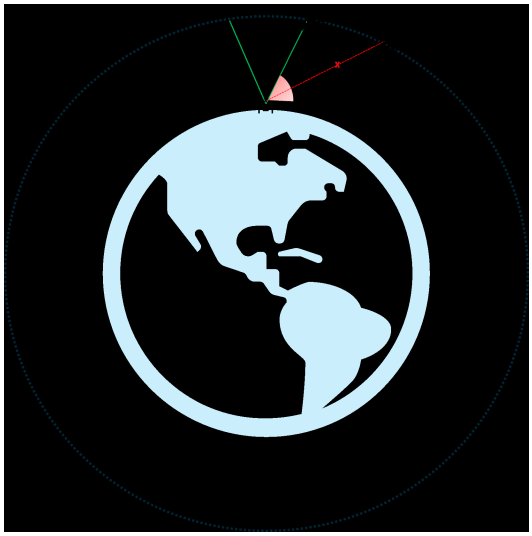

Figure 4. Visualization of the elevation mask on the drone.

5. Results

Using the methods discussed in the previous section, the link budget analysis and mobility-and-handover analysis were carried out by simulating the provided problem statement in MATLAB R2024a The results are discussed below:

5.1. Link Budget

There are four studies that were done on link budget analysis, which are mentioned below:

- The effect of weather attenuation on the received power at different elevation angles of a UAV receiver: Weather attenuation significantly impacts the quality of the communication link. By evaluating how weather conditions affect the received power at different elevation angles, the research provides insights into the robustness of

the communication link across diverse atmospheric conditions. This is essential for designing UAV communications that remain reliable in adverse weather.

- The effect of the altitude of a UAV on the link parameters: The altitude of a UAV directly influences several link parameters, such as the path loss, delay, and signal strength. Higher altitudes may facilitate a better line of sight with satellites, but they could also result in increased path losses with terrestrial base stations, as reported in [26]. Evaluating this effect allows for the optimization of UAV operating altitudes to balance the benefits of improved satellite visibility against the potential disadvantages of increased path losses with terrestrial links.
- Path loss vs. elevation angle: The path loss varies with the elevation angle due to the changing distance and propagation environment between the transmitter and receiver. This evaluation helps in understanding how the geometric configuration of a satellite and a UAV impacts the efficiency of the communication link. Optimizing the elevation angle can minimize the path loss, thereby enhancing the overall performance of the network.
- Link margin vs. elevation angle: The link margin, the difference between the received signal strength and the minimum required signal strength for acceptable performance, is a critical parameter in ensuring communication reliability. By studying how the link margin varies with elevation angle, research can determine the most reliable operational angles for UAVs. This is crucial for ensuring that UAVs maintain sufficient link margins to handle unexpected variations in signal strength due to dynamic changes in their operating environment.

5.1.1. Effect of Weather Attenuation or Received Power

To study the effect of attenuation due to weather, the received signal was analyzed for a fixed-point drone. The received signal strength is noted for every elevation angle the satellite achieves with the drone. This can be visualized using Figure 5.

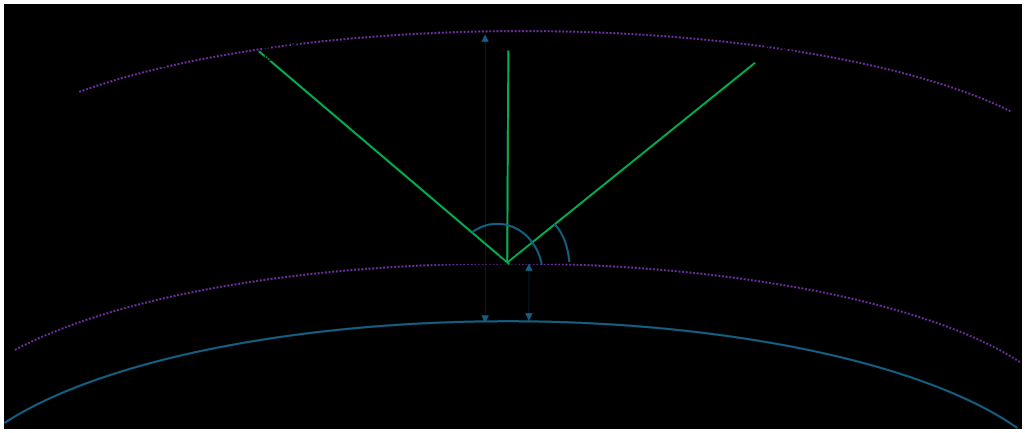

Figure 5. Visualization of analysis setup.

This analysis was carried out for three cases, namely the following:

- Free space.
- Atmospheric attenuation only.
- Atmospheric and rain attenuation.

For this analysis, the UAV was considered to be at a height of 500 m above the Earth's surface. The power received for each of the three cases mentioned above at different elevation angles from the drone can be seen in Figure 6. Since the drone has an elevation mask of 60°, the elevation angle varied from 60° to 120°.

From Figure 6, it can be inferred that the received power is reduced significantly due to atmospheric attenuation compared to the one received in free space. Rain attenuation further reduces the received power. There is a negligible loss in signal strength without

attenuations, and hence, the received power is approximately constant with varying elevation angles. Similarly, the carrier-to-noise ratio or SNR variation due to various attenuation is shown in Figure 7. From the results, we can infer that weather effects significantly impact the signal quality. Bad weather may result in a lower range for the satellite. The signal quality would be best when the elevation angle would be 90 degrees, i.e., the satellite, the UAV, and the center of the Earth would fall in a straight line.

Latency and FSPL do not vary with the attenuation. This is because these parameters are functions of distance only. The distance between the UAV and the satellite would vary with changes in the elevation angle. The plots showing their variation with the elevation angle are shown in Figures 8 and 9, respectively.

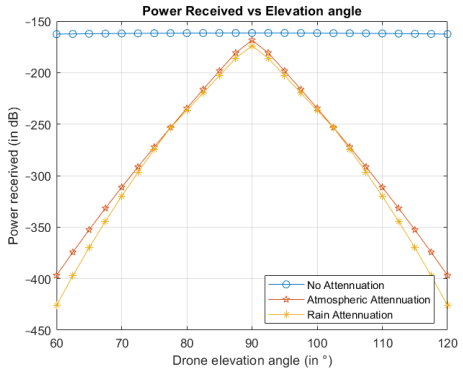

Figure 6. Received power with various attenuation.

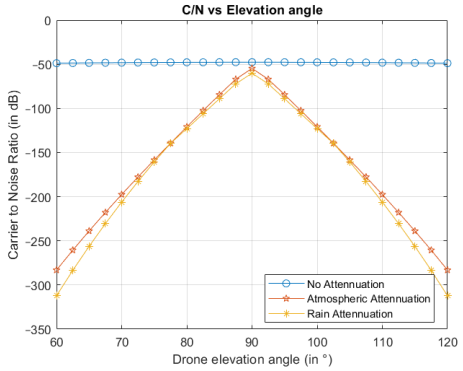

Figure 7. C/N vs. horizontal distance for different attenuations.

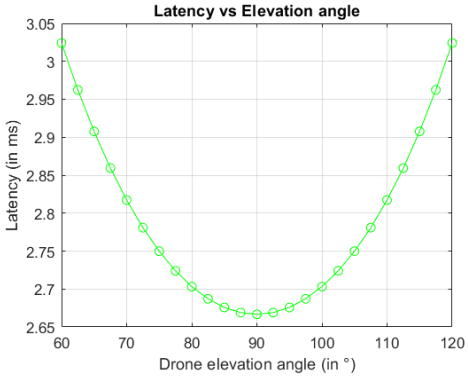

Figure 8. Latency vs. horizontal distance.

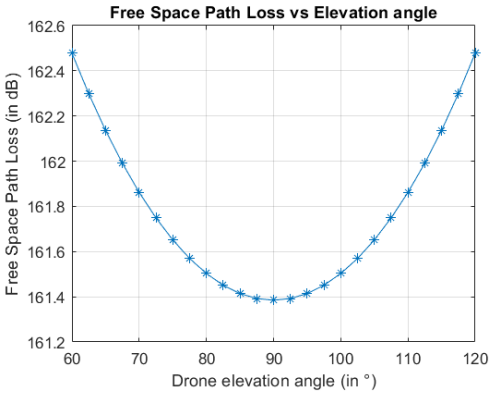

Figure 9. FSPL vs. horizontal distance.

5.1.2. Effect of Altitude of UAV on Link Parameters at a Given Speed

As discussed in the introduction, UAM requires communication systems at different altitudes. The link parameters and quality of service vary with changes in altitude. The analysis below was done while considering the power received via the UAV after rain attenuation. The link parameters vs. the distance curves at various altitudes with the UAV traveling at 45 m/s are shown in the figures below. The Doppler effect was considered when evaluating the drone's relative velocity, considering the satellite's orbit velocity.

Figure 10 shows the variation in the received power as we increase the altitude. It is evident from the figure that, as we increase the altitude, more power is received. This is due to fewer losses along the path, as the path becomes shorter. It can be noted that, beyond the altitude of 2000 m (above the cloud altitude), the change in the received signal strength is much less. This happens since rain attenuation is no longer a factor beyond 2000 m in altitude.

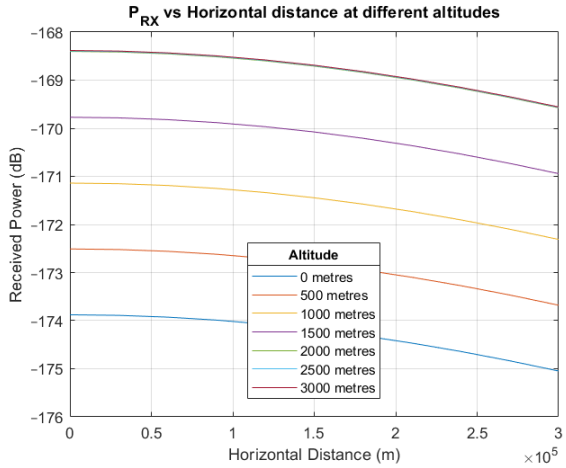

Figure 10. Received power vs. horizontal distance at different altitudes.

Figure 11 shows the variation in FSPL as we increase the altitude. From the result shown in the figure, we can infer that the free path loss decreases with an increase in altitude, while it increases as the UAV moves laterally away from the satellite at a constant altitude. This is because the distance between the satellite and the UAV decreases. Naturally, this trend is the opposite of what was observed for ground base stations in [26].

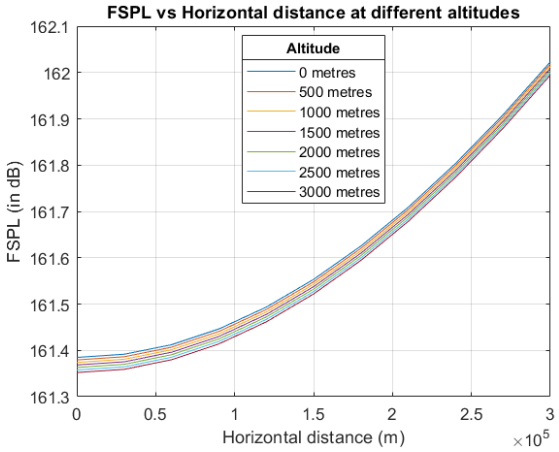

Figure 11. FSPL vs. horizontal distance at different altitudes.

The carrier-to-noise ratio (SNR) and latency were calculated and plotted against the horizontal distance for different altitudes. The results are shown in Figure 12 and Figure 13, respectively. The SNR would decrease as the UAV moved closer to the satellite, and there would be less noise as you moved closer to the source of the signal. Latency drops as the UAV moves to a higher altitude in the case of satellites as the distance between the UAV and the satellite is reduced. These results show that the link budget parameters for satellite communications exhibit opposite trends when compared to ground base stations [26]. This is solely due to the direction of the source of the signal. When the altitude of the UAV is increased, it moves closer to the satellite but away from ground base stations.

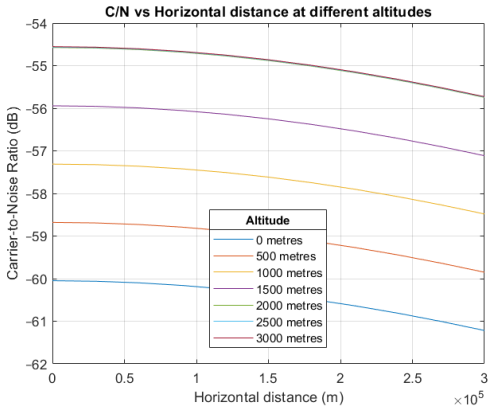

Figure 12. C/N vs. horizontal distance at different altitudes.

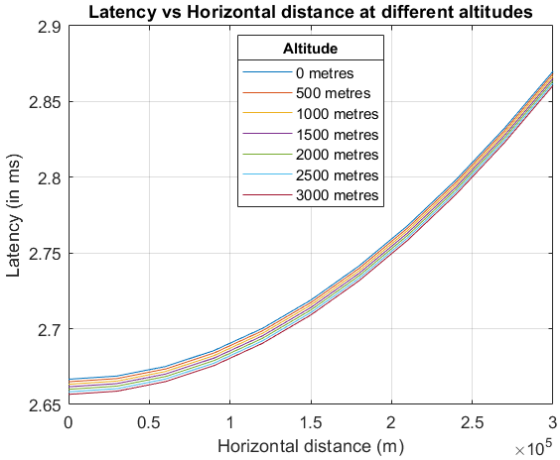

Figure 13. Latency vs. horizontal distance at different altitudes.

From these figures, it can be noted that both C/N and latency decrease with an increase in altitude. One of the factors important to note here is that, due to the vertical polarization of the rain attenuation, the power loss is more in the vertical direction as compared to the horizontal direction, and hence, for the given problem statement, a UAV moving vertically up is more likely to lose its connection to the base station compared to a UAV moving horizontally due to rain.

5.1.3. Path Loss vs. Elevation Angle

Figure 14 shows the path loss of the signal, considering the free-space loss, weather attenuation, and Doppler effect. The minimum path loss occurs when the elevation angle is 90 degrees. Hence, the best signal quality is achieved when the satellite is directly above the UAV. As the satellite moves away from the UAV, the path loss gradually increases.

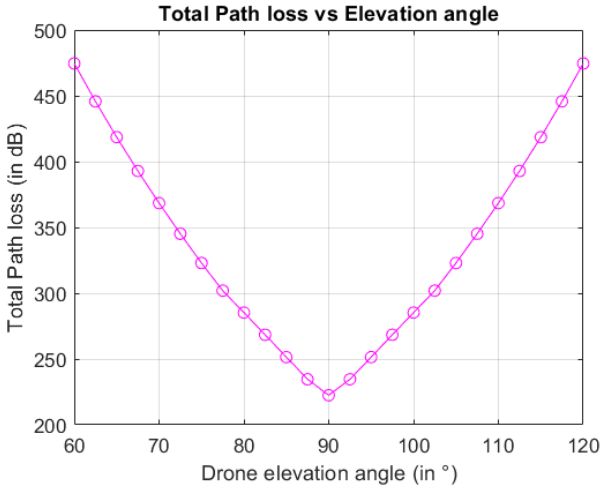

Figure 14. Path-loss vs. horizontal distance.

5.1.4. Link Margin

For the given minimum C/N required (i.e., −120 dB), and an altitude of 500 m, the link margin was calculated and is shown in Figure 15. From the figure, we observe that the link margin is not positive throughout the change in the elevation angle from 60° to 120°. The 6G communication link can be maintained only when the link margin is positive. Hence, it can be said that, even though the satellite is in the visible range of the receiver drone, it is not always possible to establish a 6G link. The elevation angle needs to be roughly between 80 and 100 to maintain a 6G communication link ($\theta_{lim-elevation} = \{80°, 100°\}$).

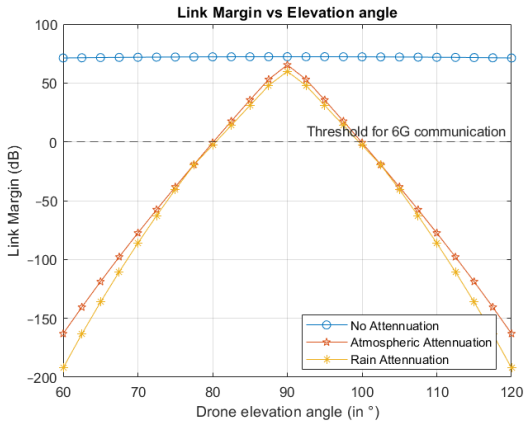

Figure 15. Link margin vs. horizontal distance.

From the link margin, the range of the 6G satellite–terrestrial network can be determined. The elevation angle and the range where the link margin is positive can be related using the following equations. Figure 16 can be used to understand the calculations.

$$\theta = 90^{\circ} - \theta_{lim-elevation} \tag{20}$$

$$\alpha = \theta - \arcsin\left(\frac{R_e}{R_{sat}}\sin\theta\right) \tag{21}$$

$$Range_{6G} = R_e(2\alpha) \tag{22}$$

The above equations, Equations (20)–(22), were used to calculate the range of the 6G satellite network at 250 km on the ground.

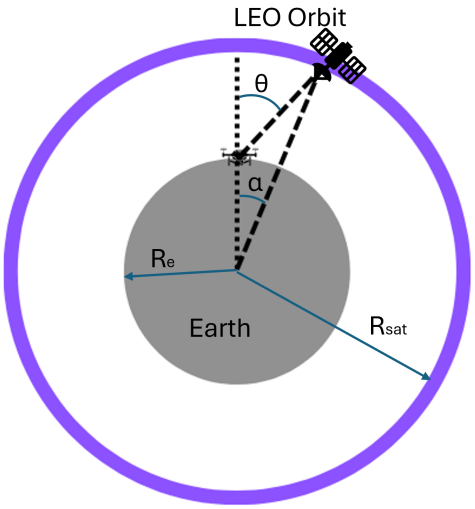

Figure 16. Calculation of range of 6G satellites.

5.2. Mobility and Handover Analysis

The handover analysis was carried out for a UAV traveling at a constant altitude of 500 m. The UAV communication link has to be handed over between various ground stations and satellites along its path to maintain constant connectivity. This is shown in Figure 17.

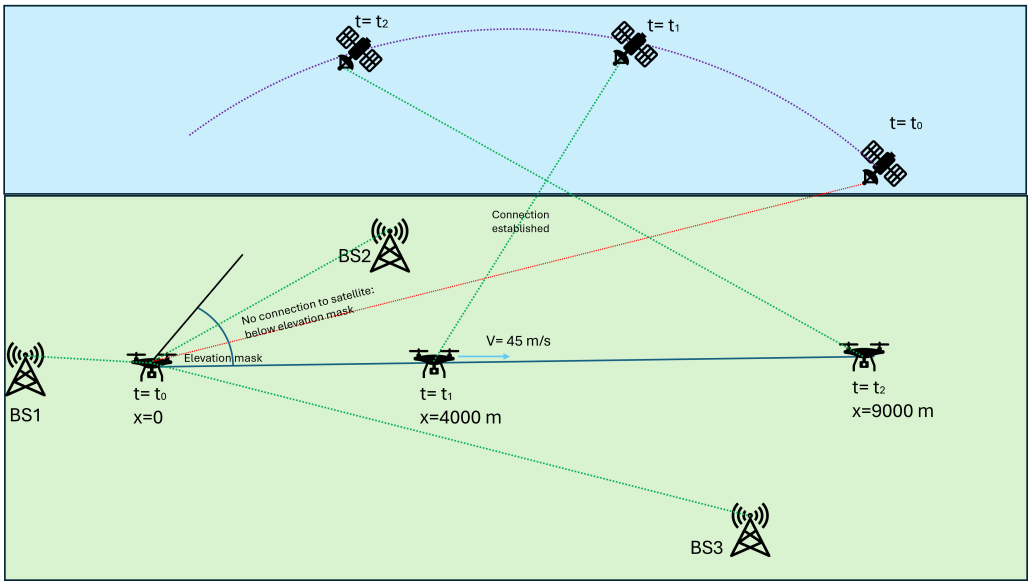

Figure 17. Visualization of use case considered for analysis.

The assumptions for the ground base stations are as follows (Table 2). The coordinates (−1000, 0, 0), (2000, 800, 0), and (9000, −3000, 0) represent a deliberate placement of base stations across a broad geographic area. This distribution allows for the assessment of UAV communication effectiveness over varying distances and directional paths, which is crucial for testing the network's handover protocols and signal continuity. By setting the base stations at these points, there is an overlap of coverage areas, which is essential for evaluating the handover algorithms.

The 6G terrestrial base station is assumed to have 38 dBm transmitter power [34]. The handover analysis was carried out along the UAV path, and the active base station is shown in Figure 18.

Table 2. Initial values for handover analysis: Case-1.

Parameter	Value
BS1 coordinates	−1000, 0, 0
BS2 coordinates	2000, 800, 0
BS3 coordinates	9000, −3000, 0
Frequency (f)	3.5 GHz
UAV initial position (m)	0, 0, 500
UAV final position (m)	9000, 0, 500
UAV velocity	45 m/s
Attenuation constants	Same as Table 1
Power BS1	8 dB (6G ground station) [34,35]
Power BS2	8 dB (6G ground station)
Power BS3	8 dB (6G ground station)
Signal threshold	−120 dB (assumed for 6G)

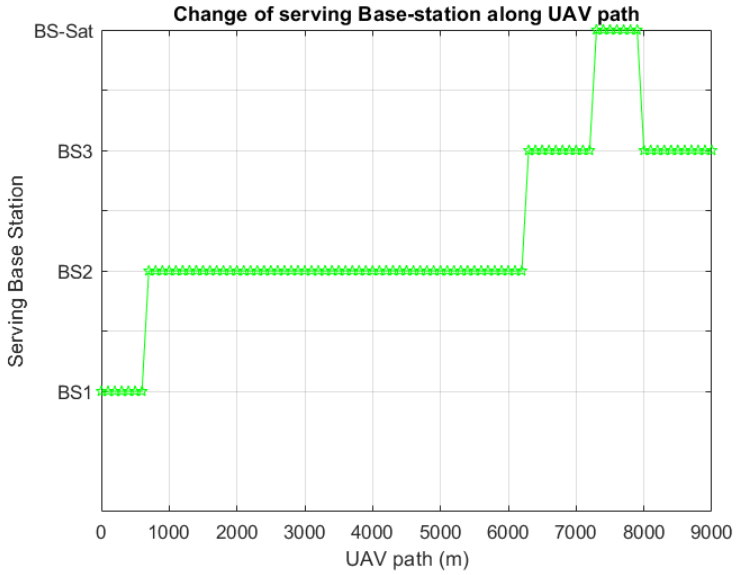

Figure 18. Serving base station along the UAV path.

Figure 18 shows that there are four handovers taking place along the UAV path. Serving BS = 0 means the signal is lost, as the RSS is below the signal threshold. For the considered use case, since the serving base station is never zero, constant connectivity is maintained throughout the flight path. The received signal strength (RSS) of the received signal from each of the stations can be observed in Figure 19.

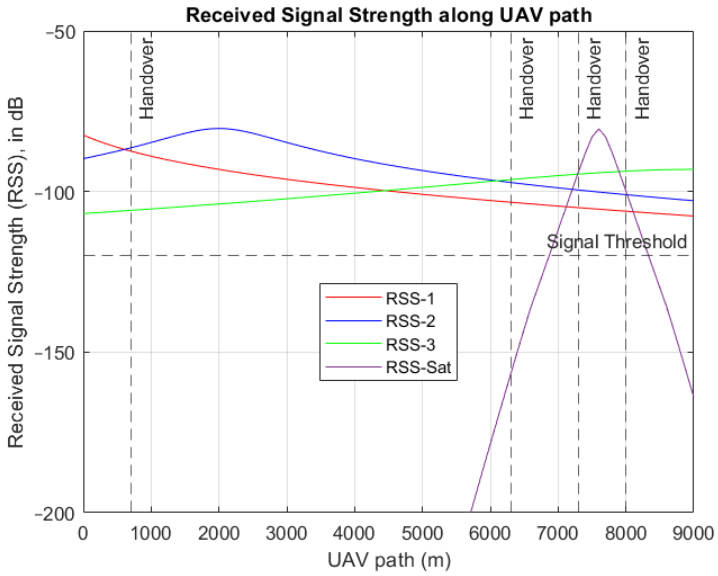

Figure 19. Received signal strength along UAV path.

From Figure 19, it can be seen why there are four handovers. The received signal strength of the new signal is stronger than the sum of the old signal strength and its entropy at that position. The maximum signal strength received via the drone is observed to be higher than the signal threshold of −120 dB, considered for 6G connectivity. Another interesting inference from the graph is that, even though the satellite comes into the visible range at x = 4000 m, the signal strength is not enough to sustain 6G connectivity.

6. Discussion

The assumptions made about drone (UAV) flight conditions in this study, including the use of only one satellite for comparison, constant-altitude travel in a straight line, and 2D analysis, significantly shape the interpretation and applicability of the results. Each of these assumptions simplified the real-world complexities of UAV operations and satellite communications, which may have influenced the validity and generalization of the findings.

The use of a single satellite to compare with ground stations limited the analysis to a scenario where interference from other satellites or overlapping signals was non-existent. In reality, multiple satellites might be available, offering alternative communication links and affecting the signal quality due to interference. Relying on a single satellite may result in an overestimation of the signal reliability and strength, as it does not account for potential satellite malfunctions or suboptimal positioning relative to the UAV. The results might suggest better connectivity or fewer handovers than might actually occur in a multi-satellite environment where handover decisions could be more dynamic and complex.

For the link budget, a straight-line path for the UAV was assumed. This may have led to an oversimplification of the analysis, potentially making the handover algorithms less effective in adaptive or complex flight patterns encountered in practical applications. The UAV, the satellite, and the center of the Earth were assumed to be in the same plane, which meant that the analysis was 2D. The exclusion of 3D spatial factors could have led to inaccuracies in predicting the signal strength and handover performance, making the results less applicable to scenarios where the UAV's relative altitude and geographic positioning vary significantly from the satellite.

While the study's assumptions streamlined the modeling and analysis, making the complex problem of UAV-to-satellite communications more tractable, they introduced limitations that could affect the practical application of the research findings. Recognizing these limitations is crucial for interpreting the results and for considering further research that incorporates more dynamic and realistic flight patterns and satellite environments. This

acknowledgment also guides the development of more robust and adaptive communication systems that can handle the complexities of real-world UAV operations.

7. Conclusions

The link budget analysis achieved a positive link margin for the given data, indicating successful communication between the transmitter and the UAM vehicle. The effect of velocity and altitude on various link parameters and quality of service metrics i.e., latency, were also studied. This study was done while considering different weather attenuations. A loss model was formulated, taking all the losses into account.

In the second part, a study on mobility and handover analysis was carried out for a UAM vehicle moving on a straight-line path, using the entropy method and considering three base stations. The signal strength at the UAV from three ground base stations and one satellite base station along the flight path was studied. It was observed that the satellite connection could provide 6G connectivity for only about 250 km on the ground at a time instant. Hence, a larger number of satellites would be required in orbit to provide a 6G terrestrial network to the whole world. The number would depend on the type of service the 6G network aimed to provide.

This work contributes to the virtual knowledge bank for researchers working toward the successful implementation of robust communication systems for urban air mobility (UAM). This study highlights the effects of altitude and weather on communication systems. It also proves a methodology for signal handover using the entropy method. This study will be useful for use cases involving UAVs in remote areas, such as medical deliveries, mapping, etc.

8. Future Work

This paper studied the link budget for one satellite through its visible time and compared to ground base stations. In the future, various satellite constellations can be studied, adding more indicators to the entropy-weight method for handovers. These indicators can comprise capacity, data speed, and the remaining service time. More link budget parameters, like the bit error rate, can be introduced, which would delve into channel modeling for LEO SATCOM systems.

Author Contributions: Conceptualization, K.M. and S.A.-R.; methodology, K.M.; software, K.M.; validation, K.M. and S.A.-R.; formal analysis, K.M.; resources, K.M. and S.A.-R.; data curation, S.A.-R.; writing—original draft preparation, K.M.; writing—review and editing, S.A.-R.; visualization, K.M.; supervision, S.A.-R.; project administration, K.M. All authors have read and agreed to the published version of the manuscript.

Funding: This research received no external funding.

Data Availability Statement: The study's data are contained within the article.

Conflicts of Interest: The authors declare no conflicts of interest.

References

1. Thipphavong, D.P.; Apaza, R.; Barmore, B.; Battiste, V.; Burian, B.; Dao, Q.; Feary, M.; Go, S.; Goodrich, K.H.; Homola, J.; et al. Urban Air Mobility Airspace Integration Concepts and Considerations. In Proceedings of the 2018 Aviation Technology, Integration, and Operations Conference, Atlanta, GA, USA, 25–29 June 2018; p. 3676.
2. Ertürk, M.C.; Hosseini, N.; Jamal, H.; Şahin, A.; Matolak, D.; Haque, J. Requirements and Technologies Towards Uam: Communication, Navigation, and Surveillance. In Proceedings of the 2020 Integrated Communications Navigation and Surveillance Conference (ICNS), Herndon, VA, USA, 8–10 September 2020; pp. 2C2-1–2C2-15.
3. Al-Rubaye, S.; Conrad, C.; Tsourdos, A. Communication Network Architecture with 6G Capabilities for Urban Air Mobility. In Proceedings of the 2024 IEEE International Conference on Consumer Electronics (ICCE), Las Vegas, NV, USA, 6–8 January 2024; pp. 1–6. [CrossRef]
4. Warrier, A.; Aljaburi, L.; Whitworth, H.; Al-Rubaye, S.; Tsourdos, A. Future 6G Communications Powering Vertical Handover in Non-Terrestrial Networks. *IEEE Access* **2024**, *12*, 33016–33034. [CrossRef]
5. Jiang, H.; Zhang, Z.; Wu, L.; Dang, J.; Gui, G. A 3-D Non-Stationary Wideband Geometry-Based Channel Model for MIMO Vehicle-to-Vehicle Communications in Tunnel Environments. *IEEE Trans. Veh. Technol.* **2019**, *68*, 6257–6271. [CrossRef]

6. Gui, G.; Liu, M.; Tang, F.; Kato, N.; Adachi, F. 6G: Opening New Horizons for Integration of Comfort, Security, and Intelligence. *IEEE Wirel. Commun.* **2020**, *27*, 126–132. [CrossRef]
7. Jiang, H.; Mukherjee, M.; Zhou, J.; Lloret, J. Channel Modeling and Characteristics for 6G Wireless Communications. *IEEE Netw.* **2021**, *35*, 296–303. [CrossRef]
8. Bae, J.; Lee, H.; Lee, H. A Study on Communication Technologies for Urban Air Mobility. In Proceedings of the 2022 13th International Conference on Information and Communication Technology Convergence (ICTC), Jeju Island, Republic of Korea, 19–21 October 2022; pp. 2235–2240.
9. Al-Rubaye, S.; Tsourdos, A.; Namuduri, K. Advanced Air Mobility Operation and Infrastructure for Sustainable Connected eVTOL Vehicle. *Drones* **2023**, *7*, 319. [CrossRef]
10. Al-Rubaye, S.; Tsourdos, A. Airport Connectivity Optimization for 5G Ultra-Dense Networks. *IEEE Trans. Cogn. Commun. Netw.* **2020**, *6*, 980–989. [CrossRef]
11. Warrier, A.; Al-Rubaye, S.; Panagiotakopoulos, D.; Inalhan, G.; Tsourdos, A. Interference Mitigation for 5G-Connected UAV using Deep Q-Learning Framework. In Proceedings of the 2022 IEEE/AIAA 41st Digital Avionics Systems Conference (DASC), Portsmouth, VA, USA, 18–22 September 2022; pp. 1–8. [CrossRef]
12. Ozpolat, M.; Al-Rubaye, S.; Williamson, A.; Tsourdos, A. Integration of Unmanned Aerial Vehicles and LTE: A Scenario-Dependent Analysis. In Proceedings of the 2022 International Conference on Connected Vehicle and Expo (ICCVE), Lakeland, FL, USA, 7–9 March 2022; pp. 1–6. [CrossRef]
13. Whitworth, H.; Al-Rubaye, S.; Tsourdos, A.; Jiggins, J.; Silverthorn, N.; Thomas, K. Aircraft to Operations Communication Analysis and Architecture for the Future Aviation Environment. In Proceedings of the 2021 IEEE/AIAA 40th Digital Avionics Systems Conference (DASC), San Antonio, TX, USA, 3–7 October 2021; pp. 1–8. [CrossRef]
14. Mousa, M.; Al-Rubaye, S.; Inalhan, G. Unmanned Aerial Vehicle Positioning using 5G New Radio Technology in Urban Environment. In Proceedings of the 2023 IEEE/AIAA 42nd Digital Avionics Systems Conference (DASC), Barcelona, Spain, 1–5 October 2023; pp. 1–9. [CrossRef]
15. Wang, Y.; Feng, W.; Wang, J.; Quek, T.Q.S. Hybrid Satellite-UAV-Terrestrial Networks for 6G Ubiquitous Coverage: A Maritime Communications Perspective. *IEEE J. Sel. Areas Commun.* **2021**, *39*, 3475–3490. [CrossRef]
16. Qi, W.; Wang, H.; Xia, X.; Mei, C.; Liu, Y.; Xing, Y. Research on Novel Type of Non Terrestrial Network Architecture for 6G. In Proceedings of the 2023 International Wireless Communications and Mobile Computing (IWCMC), Marrakesh, Morocco, 19–23 June 2023; pp. 1281–1285. [CrossRef]
17. El Debeiki, M.; Al-Rubaye, S.; Perrusquía, A.; Conrad, C.; Flores-Campos, J.A. An Advanced Path Planning and UAV Relay System: Enhancing Connectivity in Rural Environments. *Future Internet* **2024**, *16*, 89. [CrossRef]
18. Liu, X.; Zhang, H.; Sheng, M.; Li, W.; Al-Rubaye, S.; Long, K. Ultra dense satellite-enabled 6G networks: Resource optimization and interference management. *China Commun.* **2023**, *20*, 262–275. [CrossRef]
19. Li, X.; Zhang, H.; Zhou, H.; Wang, N.; Long, K.; Al-Rubaye, S.; Karagiannidis, G.K. Multi-Agent DRL for Resource Allocation and Cache Design in Terrestrial-Satellite Networks. *IEEE Trans. Wirel. Commun.* **2023**, *22*, 5031–5042. [CrossRef]
20. He, Y.; Ren, Y.; Zhou, Z.; Mumtaz, S.; Al-Rubaye, S.; Tsourdos, A.; Dobre, O.A. Two-Timescale Resource Allocation for Automated Networks in IIoT. *IEEE Trans. Wirel. Commun.* **2022**, *21*, 7881–7896. [CrossRef]
21. Gao, Y.; Tian, F.; Li, J.; Fang, Z.; Al-Rubaye, S.; Song, W.; Yan, Y. Joint Optimization of Depth and Ego-Motion for Intelligent Autonomous Vehicles. *IEEE Trans. Intell. Transp. Syst.* **2023**, *24*, 7390–7403. [CrossRef]
22. Baltaci, A.; Dinc, E.; Ozger, M.; Alabbasi, A.; Cavdar, C.; Schupke, D. A Survey of Wireless Networks for Future Aerial Communications (FACOM). *IEEE Commun. Surv. Tutor.* **2021**, *23*, 2833–2884. [CrossRef]
23. Zhang, Y.; Wu, Q.; Lai, Z.; Li, H. Enabling Low-latency-capable Satellite-Ground Topology for Emerging LEO Satellite Networks. In Proceedings of the IEEE INFOCOM 2022—IEEE Conference on Computer Communications, London, UK, 2–5 May 2022; pp. 1329–1338. [CrossRef]
24. Vanelli-Coralli, A.; Chuberre, N.; Masini, G.; Guidotti, A.; El Jaafari, M. *5G Non-Terrestrial Networks: Technologies, Standards, and System Design*; John Wiley & Sons, Inc.: Hoboken, NJ, USA, 2024; pp. 1–300. [CrossRef]
25. Yao, Y.; Dong, D.; Cai, C.; Huang, S.; Yuan, X.; Gong, X. Multi-UAV-assisted Internet of Remote Things communication within satellite–aerial–terrestrial integrated network. *Eurasip J. Adv. Signal Process.* **2024**, *2024*, 10. [CrossRef]
26. Whitworth, H.; Al-Rubaye, S.; Tsourdos, A. Urban Air Mobility Link Budget Analysis in 5G Communication Systems. In Proceedings of the 2023 IEEE 24th International Symposium on a World of Wireless, Mobile and Multimedia Networks (WoWMoM), Boston, MA, USA, 12–15 June 2023; pp. 400–406. [CrossRef]
27. Ozger, M.; Gódor, I.; Nordlow, A.; Heyn, T.; Pandi, S.; Peterson, I.; Viseras, A.; Holis, J.; Raffelsberger, C.; Kercek, A.; et al. 6G for Connected Sky: A Vision for Integrating Terrestrial and Non-Terrestrial Networks. In Proceedings of the Networking and Internet Architecture, Gothenburg, Sweden, 6–9 June 2023; pp. 711–716. [CrossRef]
28. Zhu, X.; Jiang, C. Integrated Satellite-Terrestrial Networks Toward 6G: Architectures, Applications, and Challenges. *IEEE Internet Things J.* **2022**, *9*, 437–461. [CrossRef]
29. Jia, Z.; Sheng, M.; Li, J.; Niyato, D.; Han, Z. LEO-Satellite-Assisted UAV: Joint Trajectory and Data Collection for Internet of Remote Things in 6G Aerial Access Networks. *IEEE Internet Things J.* **2021**, *8*, 9814–9826. [CrossRef]
30. Deb; p.K.; Mukherjee, A.; Misra, S. XiA: Send-It-Anyway Q-Routing for 6G-Enabled UAV-LEO Communications. *IEEE Trans. Netw. Sci. Eng.* **2021**, *8*, 2722–2731. [CrossRef]

31. Zhou, D.; Sheng, M.; Li, J.; Han, Z. Aerospace Integrated Networks Innovation for Empowering 6G: A Survey and Future Challenges. *IEEE Commun. Surv. Tutor.* **2023**, *25*, 975–1019. [CrossRef]
32. Basha, P.H.; Prathyusha, G.; Rao, D.N.; Gopikrishna, V.; Peddi, P.; Saritha, V. AI-Driven Multi-Factor Authentication and Dynamic Trust Management for Securing Massive Machine Type Communication in 6G Networks. *Int. J. Intell. Syst. Appl. Eng.* **2024**, *12*, 361–374.
33. MATLAB. What Is a Link Budget?—MATLAB & Simulink. Available online: https://uk.mathworks.com/discovery/link-budget.html (accessed on 16 July 2024).
34. Saarnisaari, H.; Chaoub, A.; Heikkilä, M.; Singhal, A.; Bhatia, V. Wireless Terrestrial Backhaul for 6G Remote Access: Challenges and Low Power Solutions. *Front. Commun. Netw.* **2021**, *2*, 710781. [CrossRef]
35. Cho, H.; Mukherjee, S.; Kim, D.; Noh, T.; Lee, J. Facing to wireless network densification in 6G: Challenges and opportunities. *ICT Express* **2023**, *9*, 517–524. [CrossRef]
36. Whitworth, H.; Al-Rubaye, S.; Tsourdos, A. Utilizing Satellite Communication to Enable Robust Future Flight Data Links. In Proceedings of the 2023 IEEE/AIAA 42nd Digital Avionics Systems Conference (DASC), Barcelona, Spain, 1–5 October 2023; pp. 1–8. [CrossRef]
37. Deng, Z.; Long, B.; Lin, W.; Wang, J. GEO Satellite Communications System Soft Handover Algorithm Based on Residence Time. In Proceedings of the 2013 3rd International Conference on Computer Science and Network Technology, Dalian, China, 12–13 October 2013; pp. 834–838. [CrossRef]
38. Wu, Y.; Hu, G.; Jin, F.; Zu, J. A Satellite Handover Strategy Based on the Potential Game in LEO Satellite Networks. *IEEE Access* **2019**, *7*, 133641–133652. [CrossRef]
39. Zhang, S.; Guo, L.; Mu, W.; Wang, J.; Liu, Y. Multi-objective Satellite Selection Strategy Based on Entropy. In Proceedings of the 2021 13th International Conference on Wireless Communications and Signal Processing (WCSP), Changsha, China, 20–22 October 2021; pp. 1–5. [CrossRef]
40. Warrier, A.S.; Al-Rubaye, S.; Panagiotakopoulos, D.; Inalhan, G.; Tsourdos, A. Entropy Weighted Method Handover for 5G-UAV Systems in Urban Environments. *EasyChair* 2021, *preprint*.
41. Zhu, Y.; Tian, D.; Yan, F. Effectiveness of entropy weight method in decision-making. *Math. Probl. Eng.* **2020**, *2020*, 3564835. [CrossRef]

Disclaimer/Publisher's Note: The statements, opinions and data contained in all publications are solely those of the individual author(s) and contributor(s) and not of MDPI and/or the editor(s). MDPI and/or the editor(s) disclaim responsibility for any injury to people or property resulting from any ideas, methods, instructions or products referred to in the content.

https://dspace.org/

Towards 6G satellite–terrestrial networks: analysis of air mobility operations

Mohanta, Krishnakanth; Al-Rubaye, Saba

2024-07-19
MDPI
https://doi.org/10.3390/electronics13142855
Mohanta K, Al-Rubaye S. (2024) Towards 6G satellite–terrestrial networks: analysis of air mobility operations. Electronics, Volume 13, Issue 14, July 2024, Article number 2855

Downloaded from a DSpace repository. https://dspace.org/